Modeling of Tyre-Clay Soil Interaction via Quasi-Static Moving Boundary Displacement Method

Xu, D.M.[1]
McGill University
Montreal, Quebec, Canada

Yong, R.N.
McGill University
Montreal, Quebec, Canada

Mohamed, A.M.O.
McGill University
Montreal, Quebec, Canada

ABSTRACT

A vehicle mobility model has been developed using energy principles and a quasi-static moving boundary displacement method. For a given condition of both tyre and terrain characteristics, the model calculates the contact length, the slip rate, the traction efficiency and the drawbar pull. The effect of tread configuration is also included in calculating the slip rate. A numerical example is given to demonstrate the capability of the new developed mode. The model's predictions are also compared with the experimental results in the laboratory tests and a good agreement is obtained.

Key Words: _vehicle mobility, tyre-soil interaction_

INTRODUCTION

The capability for evaluation and prediction of tyre-soil interactions are of common interest for both designer and user of wheeled vehicles. A number of studies have been published and various models (experimental, semi-experimental and theoretical) have been proposed by many researchers [2], [10]. In recent years, with increasing knowledge of tyre soil interaction systems, and the rapid development of numerical methods and computer techniques, more and more attention is being paid to the development of theoretical models which can adequately predict

tyre performance on soils. This is particularly essential for vehicles which have to operate on clay soil.

To develop a realistic mathematical model the following should be included: (1) mechanical behaviour of pneumatic tyres; (2) physical as well as mechanical behaviour of soil; and (3) interaction characteristics between tyre and soil.

This study presents a complete model for tyre performance on clay soil using a quasi-static moving boundary displacement method of analysis. In brief, the method works with an analysis of the displacement around the contact boundary between the loaded tyre and the supporting ground surface. The contact length is first determined so that the subsequent calculated stresses on the contact boundary can be specified. The slip rate and the traction efficiency are given as a natural outcome based on shear test data and the energy conservation principle.

THEORETICAL FORMULATION

In applying the principle of energy conservation to the evaluation of tyre performance on clay soil, the different energy components participating in the interaction between the loaded tyre and clay soil need to be calculated. The energy concept for evaluation of traction was formally introduced by Yong and Webb [6] for motion performance of rigid wheels on soft soil. Subsequently, the energy model was extended by Yong and Fattah [7], and Yong et al. [8], [9] to predict pneumatic tyre performance on soft soils.

The basic principle used in the energy model evaluates the moving performance of the tractive element (tyre) on ground surface in terms of the well-known energy balance equation:

Input energy = output energy + energy losses (1)

With the quasi-static assumption, the vehicle is assumed to move on the terrain surface at a relatively low speed so that dynamic effects (including vertical vibration of vehicle system and soil damping) can be neglected. The energy balance equation in terms of power can be written as:

$$P_{use} = P_{input} - (P_{slip} + P_{soil} + P_{tyre}) \qquad (2)$$

where: P_{use} = the useful power; P_{input} = the to-

---

[1]_The authors are respectively; Research Associate, Geotechnical Research Centre; Professor, Civil Engineering and Applied Mechanics, and Director, Geotechnical Research Centre; and Research Associate, Geotechnical Research Centre, and Adjunct Professor, Civil Engineering Department._

tal power input to wheel; P_{slip} = the power dissipated due to tyre slip; P_{soil} = the power dissipated in soil deformation, and P_{tyre} = the power dissipated in tyre deformation.

This method of mobility evaluation [4] is especially suitable for the initial stage when the vehicle begins to move on a specified terrain surface from the "at-rest" condition. It not only answers whether the vehicle can or cannot move, i.e., "go or no go" question, but also gives a reasonable estimation of vehicle mobility for the assumed conditions: (1) slow speed, and (2) no vibration effect.

Input Energy

The input energy, through the applied torque T_o on the tyre during time t_o is given by:

$$E_{input} = T_o \omega t_o \tag{3}$$

or

$$P_{input} = T_o \omega \tag{4}$$

where: E_{input} = total input energy; (kN.m. rad); P_{input} = total input power (kN.m); ω = tyre angular velocity (rad/sec); T_o = applied torque (kN.m), and t_o = time (sec).

Slip Energy

The slip (dissipated) energy due to the applied torque T_o on the tyre during time t_o is given by:

$$E_{slip} = T_o \omega t_o S \tag{5}$$

or

$$P_{slip} = T_o \omega S \tag{6}$$

where: E_{slip} = the dissipated (lost) energy due to tyre slip (kN.m.rad); P_{slip} = the dissipated power due to slip (kN.m), and S = the slip rate, which is given by:

$$S = \frac{\omega r - v}{\omega r} \tag{7}$$

where: S measures the efficiency of the transfer of the tyre rotational motion into the horizontal vehicle motion; r = rolling radius (m), and v = translational velocity (m/sec).

Soil Dissipated Energy

When the vehicle moves on the terrain surface, it continuously "loads" the undisturbed soil and hence soil will be deformed and energy will be dissipated due to soil deformation. This energy is directly related to the normal stress distribution on the contact area between tyre and terrain surface. For the terrain surface, the loading situation can be considered in terms of a distributed stress along the contact length moving at vehicular speed.

The moving boundary loading condition can be specified as follows, any concentrated point load F(kN) acting at a distance x_o from the origin of the coordinates may be described by

$$F(t) = F\delta(x - x_o) \text{ or } F < z - x_o >^{-1} \tag{8}$$

where $\delta(x - x_o)$ is the Dirac-delta function defined by:

$$\delta(x - x_o) = \lim_{\varepsilon \to 0} \begin{cases} 0 & \text{when} & x < \left(x_o - \frac{\varepsilon}{2}\right) \\ \frac{1}{\varepsilon} & \text{when} & \left(x_o - \frac{\varepsilon}{2}\right) < x < \left(x_o + \frac{\varepsilon}{2}\right) \\ 0 & \text{when} & x > \left(x_o + \frac{\varepsilon}{2}\right) \end{cases} \tag{9}$$

For the problem under consideration, the point load F and the distance x_o take the following relations:

$$F_v = b \int_{-\ell}^{\ell} \sigma(u) du \tag{10}$$

and

$$x_o = vt \tag{11}$$

where: $\sigma(u)$ = normal stress distribution along the contact length (kN/m²), ℓ = half contact length (m); b = tyre width (m); and u = distance ranges between $-\ell$ to ℓ (m). It can be noted that Eq. (10) implies that along tyre width b the stress distribution is uniform. Substituting Eqs. (10) and (11) into Eq. (8), the vertical load $F_v(t)$ is given as:

$$F_v(t) = F_v < x - vt >^{-1} = b \int_{-\ell}^{\ell} \sigma(u) du. < x - vt >^{-1} \tag{12}$$

where: x = the transverse coordinate measured from the tyre centre to a stationary reference (m), and F_v is the axial load on the wheel from the vehicle weight.

The simplification of a quasi-static assumption is to guarantee that the normal force F_v is constant, which in turn is not violated by the dynamical effects. Therefore, one can evaluate the soil dissipated energy using a simplified set of calculations. To calculate the soil dissipated energy, the normal stresses on the contact area must be calculated first. The normal stress distribution on the contact area is usually assumed as a parabolic shape according to Hertz contact theory as:

$$\sigma(u) = \frac{3F_v}{4\ell b}\left(1 - \frac{u^2}{\ell^2}\right) \text{ for } 0 \le u \le \ell \tag{13a}$$

$$\sigma(-u) = \sigma(u) \tag{13b}$$

where: Fv = the axial load on the wheel (kN0. To simplify the calculation an average normal stress σ_{av} is suggested as follows:

$$\sigma_{av} = \frac{F_v}{2\ell b} \tag{14}$$

When the vehicle moves a distance Δ_x, the energy dissipated in deforming a new undisturbed soil element takes the following form:

$$\Delta E_{soil} = \sigma_{av} b \delta_s \Delta x \tag{15}$$

where δ_s is the soil sinkage (m) as shown in Fig. 1. Substituting Eq. (14) into (15) gives

$$\Delta E_{soil} = \frac{F_v \delta_s}{2\ell} \Delta x \tag{16}$$

Furthermore, if the vehicle moves from $x_o = 0$ to $x = x_1$ as shown in Fig. 2, the total dissipated energy is given by

$$E_{soil} = \frac{F_v \delta_s}{2\ell} \int_0^{x_1} dx$$

$$= \frac{F_v \delta_s}{2\ell} x_1 \tag{17}$$

Since $x_1 = vt_1 = (1-S)\omega r t$, one obtains

$$E_{soil} = \frac{F_v \delta_s}{2\ell}(1 - S)\omega r t_1 \tag{18}$$

The corresponding dissipated power is given by:

$$P_{soil} = \frac{F_v \delta_s}{2\ell}(1 - S)\omega r \tag{19}$$

Tyre Dissipated Energy

The tyre dissipated energy can be calculated in a similar way to soil dissipated energy. The resultant equations obtained are:

$$E_{tyre} = \frac{F_v \delta_t}{2\ell}(--S)\omega r t_1 \tag{20}$$

$$P_{tyre} = \frac{F_v \delta_t}{2\ell}(1 - S)\omega r \tag{21}$$

where: δ_t = tyre sinkage (m).

Useful Energy

According to Eq. (2), (3), (6), (19) and (21), the useful energy or power can be calculated as follows:

$$P_{use} = T_o\omega - \left[ST_o\omega + \frac{F_v \delta_s}{2\ell}(1 - S)\omega r + \frac{F_v \delta_t}{2\ell}(1 - S)\right]$$

$$= \omega(1 - S)\left[T_o - \frac{F_v r}{2\ell}(\delta_t + \delta_s)\right] \tag{22}$$

Traction Efficiency

The traction efficiency η takes the following form:

$$\eta = \frac{P_{use}}{P_{in}} = (1 - S)\left[1 - \frac{F_v r}{2\ell T_o}(\delta_t + \delta_s)\right] \tag{23}$$

Drawbar Pull

It has been known that the useful power is given by the following

$$P_{use} = F_{DP} \times v \tag{24}$$

Where: F_{DP} = Drawbar pull (kN). Substituting Eq. (24) into Eq. (22), the drawbar pull takes the following expression

$$F_{DP} = \frac{\omega(1 - S)}{v}\left[T_o - \frac{F_v r}{2\ell}(\delta_t + \delta_s)\right]$$

$$= \frac{T_o}{r} - \frac{F_v}{2\ell}(\delta_t + \delta_s) \tag{25}$$

The drawbar pull presented by Eq. (25) is for the force required to mobilize the traction forces minus the motion resistance of the wheel. It can be seen that as the input torque increased the drawbar pull increased and the drawbar pull is not a function of the slip rate. At a given constant tyre rational velocity ω, the horizontal translation velocity v is affected by slip rate S. At $S = 0$, $v = \omega r$, while at $S = 100\%$, $v = 0$. Furthermore as the input torque on the wheel increases, the slip increases. At certain limit of torque values, the slip reaches 100% and the vehicle is not able to move because the soil loses its shear resistance. At the same time, the attached drawbar pull F_{DP} reaches maximum value at $S = 100\%$. However, this force is "handicapped", with no ability to do any useful work (as the vehicle does not move). Based on such observation, it is wise to take the constant velocity ωr as observational base and express the useful power P_{use} as:

$$P_{use} = F_{TF} \times \omega r \qquad (26)$$

where F_{TF} = tractive force (kN), which is the force capable of doing useful work. Substituting Eq. (26) into Eq. (22), the following expression for the tractive force can be obtained

$$F_{TF} = (1 - S)\left[\frac{T_o}{r} - \frac{F_v}{2\ell}(\delta_t + \delta_s)\right] \qquad (27)$$
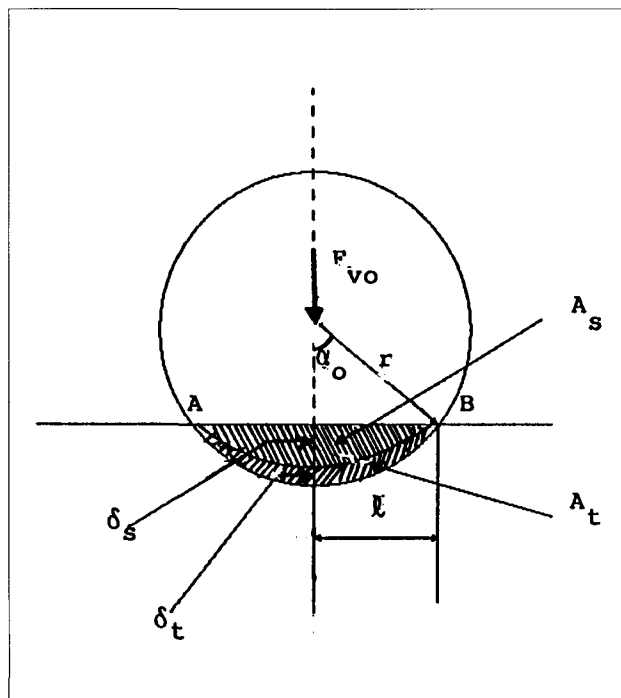

Figure 1. Geometric Representation of Soil and Tyre Compression Areas.

It can be seem from Eq. (27) that when the slip rate equals zero, the tractive force reduces to the same expression presented by Eq. (25). Furthermore, when the slip rate equals 100%, the tractive force is reduced to zero.

PARAMETER CALCULATION

The following parameters: (1) half contact length ℓ; (2) soil sinkage δ_s; (3) tyre sinkage δ_t; and (4) the slip rate S need to be calculated.

(1) Contact Length

Since both the tyre and the soil are assumed to be deformable, curve AB, as shown in Fig. 1, is the resultant contact profile which represents a compatible displacement curve in the final state after the load F_v is applied. The curve AB depends on both tyre and soil compression characteristics. Two extreme cases as shown in Fig. 3 can be discussed: (1) the soil can be considered as a rigid surface, hence the resultant curve AB is a line as shown in Fig. 3a, and (2) if one considers the tyre as a rigid disk, the resultant curve AB is a part of the tyre circumference as shown in Fig. 3b. The real situation is somewhere in between the two extreme cases.

Let us compare the contact length $2\ell_1$ (Fig. 3a) and $2\ell_2$ (Fig. 3b), in the case that the tyre size and the inflation pressure are the same but one is rigid terrain while the other is a deformed terrain. The conclusion can be reached that $2\ell_1$ is larger than $2\ell_2$. Since the terrain is deformable, it allows the tyre to sink more. The spring constant of two springs connected in series is always less than that of either spring taken individually. That is why one cannot just take the tyre compression test data to obtain the contact length without considering the terrain characteristics.

The vertical displacement of the terrain on the surface and the normal stress distribution σ are shown in Figs. 3c and 3d respectively. $\Delta_s(x)$ represents the vertical displacement of the soil contact surface at x position, while $\Delta_t(x)$ represents the vertical displacement of the tyre. At $x = 0$, $\delta_s = \Delta_s(0)$ and $\delta_t = \Delta_t(0)$, which are shown in Fig. 3c. The ratio δ_s/δ_t is a measure of the relative stiffness between the tyre and the terrain. If the terrain is extremely soft, the ratio is infinity. On the other hand, if the terrain is extremely stiff, the ratio is zero.

Hertz theory has been widely used to calculate the contact length by many authors. The subsequently obtained contact length, which based on preassumed displacement field, yields the following approximate relation

$$\ell = \left[\frac{4 F_v r}{\pi} \left(\frac{1 - v_s^2}{E_s} + \frac{1 - v_t^2}{E_t} \right) \right]^{\frac{1}{2}} \qquad (28)$$

where: E_s and E_t modulus of elasticity for soil and tyre respectively, and v_s and v_t = poisson's ratio for soil and tyre respectively. Since, neither soil nor tyre are elastic, one has to search for a new method to specify the displacement relations between δ_s and δ_t which characterize soil and tyre stiffness.

To determine the shape of the curve AB, one has to search for a technique which includes specification of both soil and tyre characteristics. The characteristics of both soil and tyre are represented in terms of soil sinkage δ_s and tyre deformation δ_t. The relationship between A_s and A_t, where A_s and A_t are the soil and tyre deformed areas in a vertical section respectively as shown in Fig. 2, is given by:

$$A = A_s + A_t$$
$$= r^2 \left(\alpha_o - sin\alpha_o \cos\alpha_s \right) \quad (29)$$

where: α_o = an angle which characterizes half contact length as shown in Fig. 1. Based on the geometrical representation in Fig. 1, the following relationships can be obtained:

$$\ell = r sin\alpha_o \qquad (30)$$

and

$$\delta = \delta_s + \delta_t = r - r cos\alpha_o$$
$$= r - \sqrt{r^2 - \ell^2} \qquad (31)$$

Eq. (29) can be written as follows:

$$A = A_s + A_t$$
$$= r^2 \left(\alpha_o - \frac{sin2\alpha_o}{2} \right) \qquad (32)$$

when α_o is small

$$sin2\alpha_o = 2\alpha_o - \frac{(2\alpha_o)^2}{2} + ..., \qquad (33)$$

and

$$cos\alpha_o = 1 - \frac{\alpha_o^2}{2} + ... \qquad (34)$$

Substituting Eq. (33) into Eq. (32), the following relations can be obtained:

$$A \approx r^2 \left(\alpha_o - \frac{1}{2} \left(2\alpha_o - \frac{4\alpha_o^2}{2} + ... \right) \right)$$
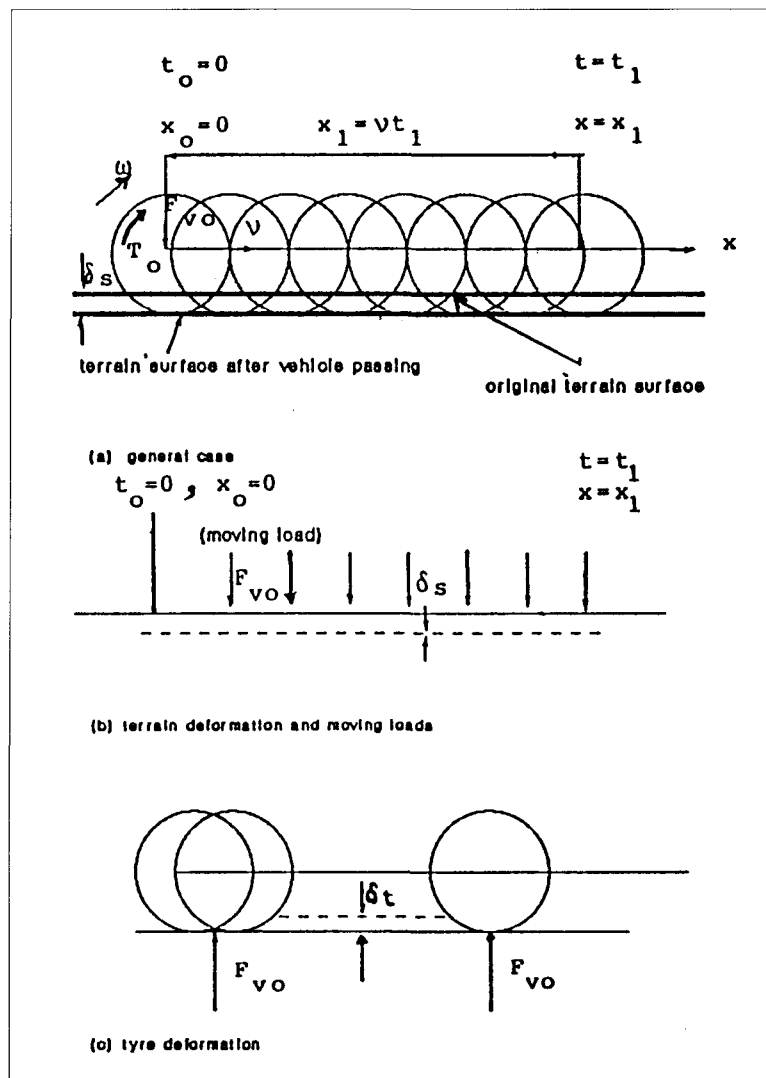$$\approx \alpha_o^2 r^2 \qquad (35)$$

Figure 2. Geometric Representations of Moving Loads, Soil Deformation and Tyre Deformation.

Substituting Eq. (34) into Eq. (31), the following relation can be obtained:

$$\delta \approx r\left(1-\left(1-\frac{\alpha_o^2}{2}\right)\right) \approx \frac{1}{2}r\alpha_o^2 \qquad (36)$$

From Eqs. (35) and (36), the relationship between A and δ can be expressed as follows:

$$A = 2r\delta \qquad (37)$$

Since A is proportional to δ, A_s and A_t can be assumed to be proportional to δ_s and δ_t respectively. The relationship can be written as follows:

$$\frac{A_s}{A_t} = \frac{\delta_s}{\delta_t} \qquad (38)$$

With the aid of Eqs. (29), (31), and (38) the soil and tyre deformed areas can be obtained as follows:

$$A_s = \frac{\delta_s}{\delta}A \qquad (39)$$

and

$$A_t = \frac{\delta_t}{\delta}A \qquad (40)$$

The tyre compression area A_t can be calculated from the tyre compression test data on a rigid surface. From a tyre compression test, one obtains a relationship between the applied load F_v and corresponding deformation of the tyre Δ_t. Since A_s is equal to zero for the case of rigid surface, the area A_t can be calculated from Eq. (29). It can be seen that due to variations in the applied load F_v the corresponding α_o as well as A_t will be changed. Therefore, a relationship between applied load F_v and the calculated areas A_t can be generated. From the generated curve at $F_v = F_{vo}$ the value A_{to} can be defined.

In a similar way, from compression tests data of a rigid tyre on soil, one obtains a relationship between the applied load F_v and the soil deformation, Δ_s. From Eq. (29), A_s can be calculated for various applied loads, and hence, a relationship between F_v and A_s can be obtained. At $F_v = F_{vo}$ the value of A_{so} can then be defined. The total area A_o as well as the corresponding angle α_o at $F_v = F_{vo}$ can be calculated from Eq. (29). The contact length can be calculated from Eq. (31). From the preceding method of calculation it can be seen that: (1) the effect of tyre and soil stiffness on the calculated contact length have been taken into account; (2) the contact length is directly related to the vertical displacement not the stress, and (3) there is no need to assume a parabolic normal stress distribution on the contact length as required for Hertz theory.

(2) Tyre and Soil Deformations

Once the contact length ℓ is calculated, the total deformation δ can be obtained from Eq. (31). The tyre and soil deformations δ_{to} and δ_{so} re-

(a) Contact Length A,B,for Soft Tyre and Rigid Terrain

(b) Contact Length A and B for Rigid Tyre and Soft Terrain

(c) Displacements $\Delta_s(x)$ and $\Delta_t(x)$

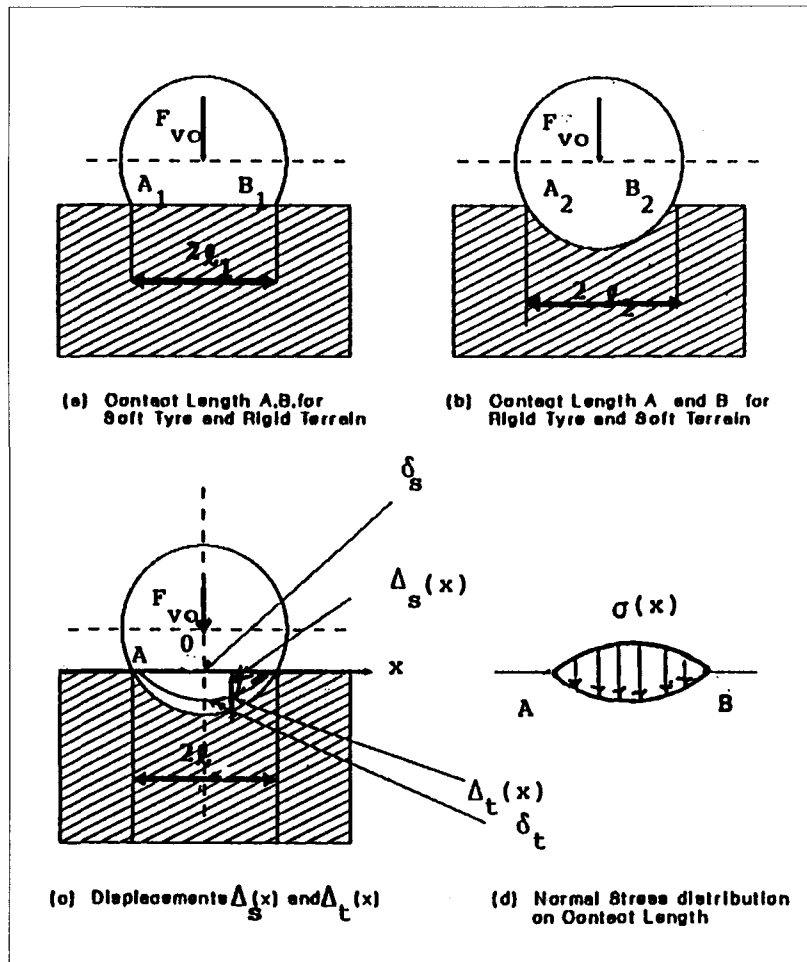(d) Normal Stress distribution on Contact Length

Figure 3. Schematic Diagram Showing Contact Length, Displacement and Normal Stress Distribution on contact Length.

spectively, at $F_v = F_{vo}$ can then be calculated from Eqs. (39) and (40).

It can be seen that the contact length is directly related to the displacements of both soil and tyre. In addition, the compression characteristics of both soil and tyre are used in a direct way to calculate the tyre and soil deformations as well as the contact length.

(3) Slip rate, S

In the original sense, slip rate S is defined as represented by Eq. (7). If the rotation of the tyre is completely transferred to a horizontal motion, $v = \omega r$ and $S = 0$. This situation requires that soil is very stiff. However, in case of soft soils, a backward movement of the soil takes place due to the induced shear stresses. In order to calculate the slip rate, direct shear tests on the specified clay soils are required. The reduction of data from direct shear test into slip rate of a tyre can proceed as follows:

(a) For a circular sample in a direct shear test, the sheared area, i.e., the contact area can be expressed as:

$$A_{sh} = \frac{\pi}{4} d_{sh}^2 \qquad (41)$$

where: A_{sh} and d_{sh} = cross sectional area and diameter for the tested sample in the direct shear test.

(b) The equivalent contact length, L, for a tyre with width (b) is:

$$L = \frac{\pi d_{sh}^2}{4b} \qquad (42)$$

(c) Assuming that a wheeled vehicle moves a circumferential distance L during the forward movement of the vehicle, a horizontal backward movement U of the soil due to shear stresses is induced. The slip rate S can then be obtained as follows:

$$S = \frac{U}{L} = \frac{4Ub}{\pi d_{sh}^2} \qquad (43)$$

(d) Eq. (43) is valid only for smooth tyres. To include the effect of treads, one has to calculate the effect of soil-soil and rubber-soil contact and their ratios. Since the tyre has a unique shear displacement, U, the following condition has to be satisfied:

$$\xi_s \tau_s + \xi_r \tau_r = \tau_{av} \qquad (44)$$

where: τ_{av} = average shear stress on the contact area which is given by

$$\tau_{av} = \frac{T_o}{2b\ell r}; \qquad (45)$$

ξ_r and ξ_s = fractions of treaded and nontreaded areas respectively, and τ_r and τ_s = the developed shear stresses at the contact areas for rubber-soil and soil-soil respectively.

(e) From direct shear experimental data, the relationships between τ_s vs U_s and τ_r vs U_r can be obtained and represented by the following hyperbolic relationships [3]:
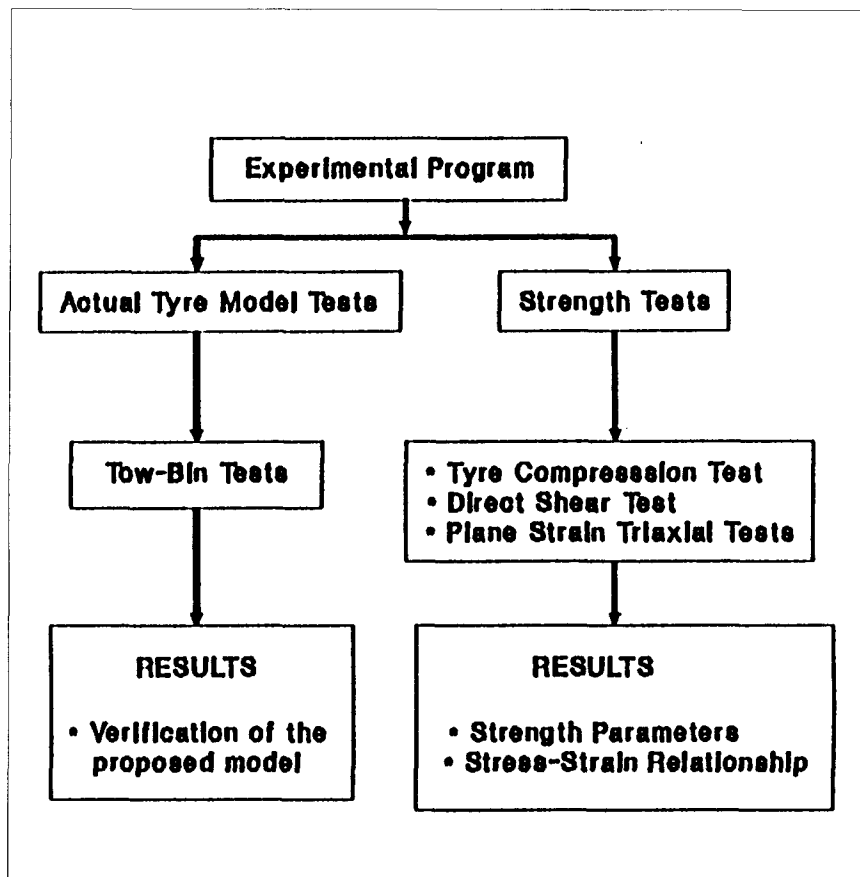

Figure 4. Main Test Arrangements Together with Test results Anticipated.

$$\tau_s = \frac{U_s}{A_s + B_s U_s} \qquad (46)$$

and

$$\tau_r = \frac{U_r}{A_r + B_r U_r} \qquad (47)$$

where: $A_s B_s A_r$ and B_r are material parameters at $\sigma = \sigma_{av}$. In physical meaning, A represents the inverse of the initial modulus of elasticity, while B represents the inverse of the ultimate shear strength. These parameters can be obtained from interpolation of both soil-soil and rubber-soil direct shear test data.

(f) Substituting Eqs. (46) and (47) into Eq. (44), one obtains the following expression for shear displacement U:

$$\tau_{av} = \zeta_s\left(\frac{U_s}{A_s + B_s U_s}\right) + \zeta_r\left(\frac{U_r}{A_r + b_r U_r}\right) \qquad (48)$$

For tyre movement on soil, the total backward movement U is equal to both U_s and U_r i.e.

$$U = U_s = U_r \qquad (49)$$

Substituting Eq. (49) into Eq. (48), the following expression for backward movement U is given:

$$U = \frac{(A_s + B_s U)(A_r + B_r U)\tau_{av}}{(A_r + B_r U)\xi_s + (A_s + B_s U)\xi_r} \qquad (50)$$

EXPERIMENTAL PROGRAM

The experimental ram is designed to be a continuation of McGill's Geotechnical Research Centre research program. The main test arrangement are presented in Fig. 4 together with the test results anticipated. In essence, the experimental work which was performed can be categorized into mainly two major divisions, namely:
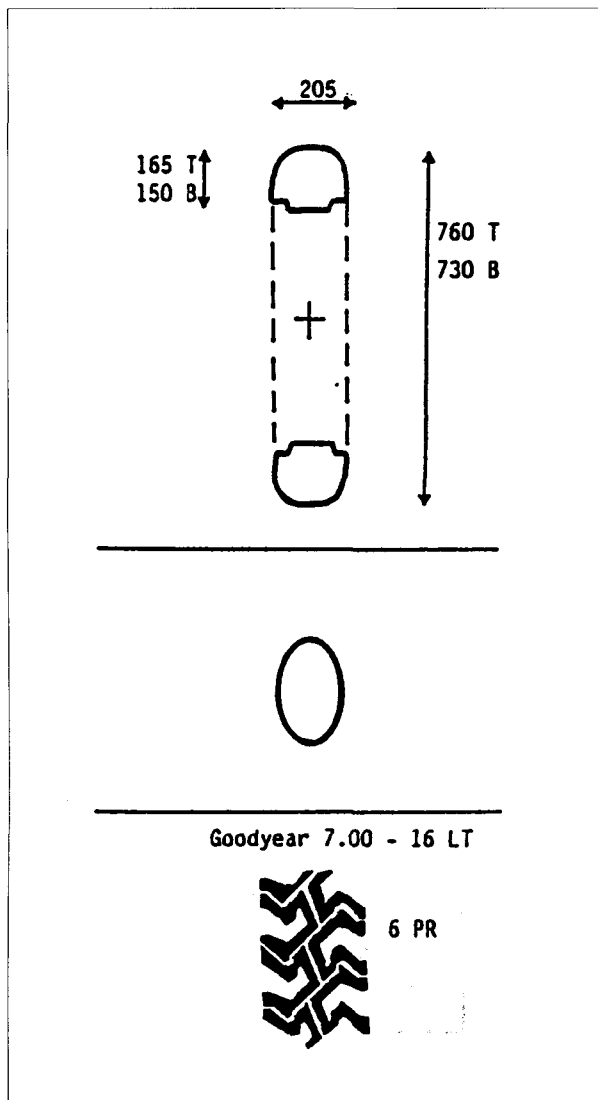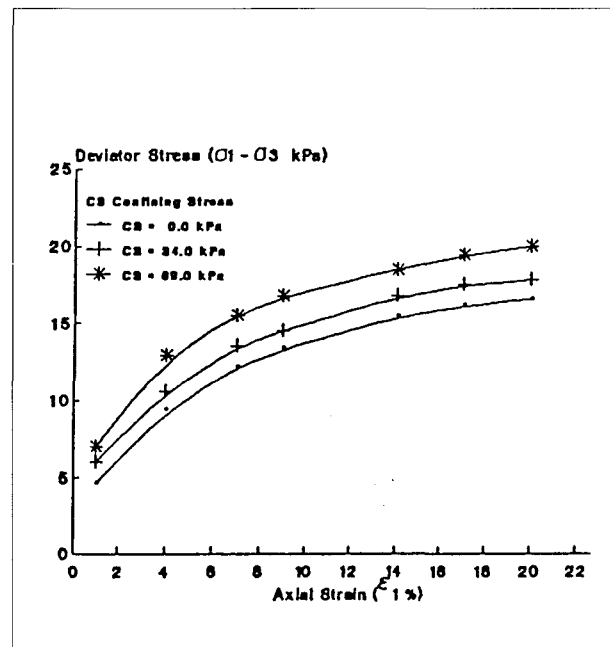
Figure 5. Tested Actual Model Tyre.

Figure 6. Stress-Strain Curves of Kaolinite Clay Under Plain-Strain Tiraxial Tests.
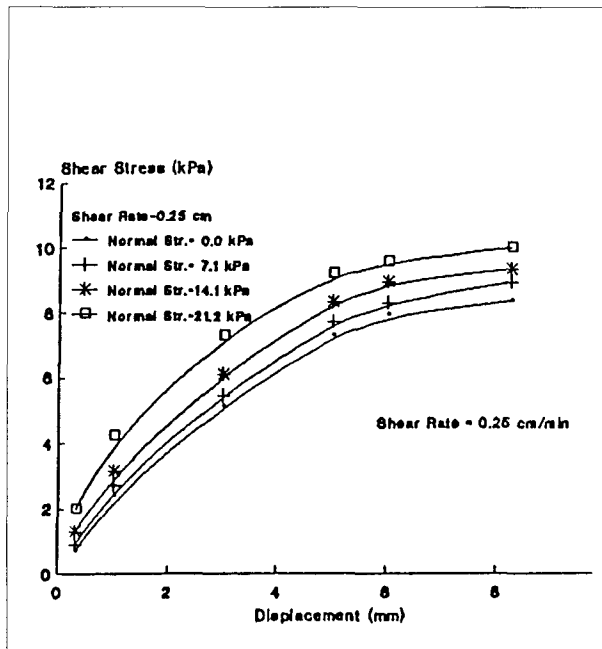
Figure 7. Shear Stress — Displacement Relationship for the Soil-to-soil Mode.
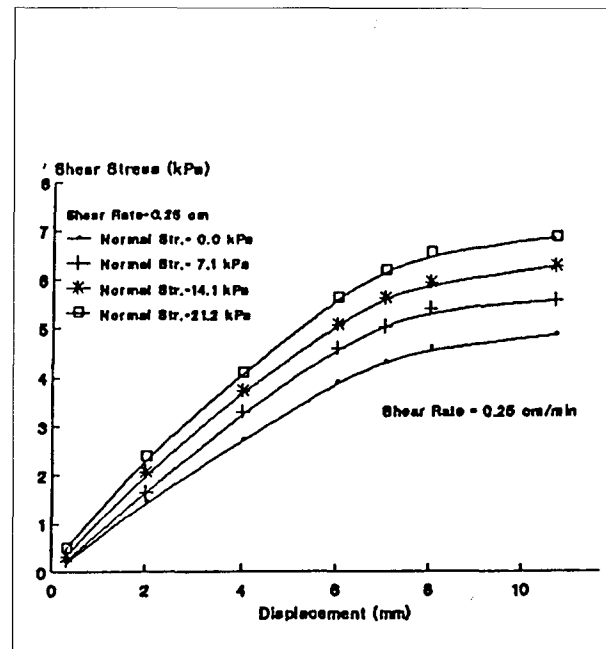

Figure 8. Shear Stress — Displacement Relationship for the Rubber-to-soil Mode.

1. Two-bin Tests – where actual tyre models were tested in the soil bin to validate the proposed model. The details of the test facilities are reported by Boyd and Windisch [1]. Fig. 5 shows the tested actual model tyre with its dimensions.
2. Strength Tests – this division can be divided into two parts:
   a. Tyre-Soil Interface Strength Tests – where the tyre-soil interface shear strength characteristics were tested using the direct shear tests for different types of interface (soil-to-soil and rubber-to-soil).
   b. Soil Strength Tests – where soil specimens with the same properties as those in the soil bin were tested in order to determine the stress-strain relationships.
   c. Tyre Strength Tests – where Goodyear 7.00-16LT (treaded) tyre with 34.5 kPa, 103.4 kPa, and 310.4 kPa inflation pressures were tested in order to determine vertical load-vertical axle deflection relationships on a rigid surface.

Soil Properties

Soft kaolinite clay which was nearly saturated (95% saturation) was used in the present experimental program. The physical properties of the soft kaolinite clay are: (1) Liquid limit L.L. =54.5%, (2) Plastic Limit P.L. =37.5%, and (3) specific gravity of solids = 2.62.

Triaxial Tests

The kaolinite clay was prepared and cut into prismatic specimens (50 x 38 x 108 mm) for triaxial testing. Confining pressures of 0, 34, and 69 kPa were used and the rate of σ_1 application was 2.5 mm/min. A plane strain condition was maintained during the
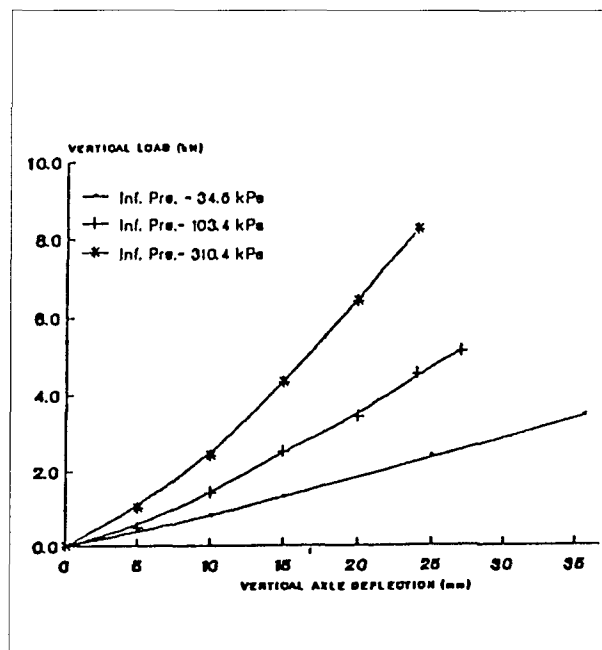

Figure 9. Shear Stress — Displacement Relationship for the Goodyear 7.00-16LT (treaded) on a Rigid Surface.

triaxial tests. The stress-strain relationships are shown in Fig. 6.

Direct Shear Tests

Two types of direct shear tests were performed. The first type was a conventional direct shear test, referred to as a soil-soil shear mode, while the second test type was conducted with the upper part of the shear box consisting of a specimen of rubber material simulating the tyre material, referred to as a rubber-soil shear mode. The first test simulates the slip condition at the tyre-soil interface where slip causes shear separation within the soil, i.e. soil-soil slip. The second test condition studies slip separation between the tyre and soil, assuming that slip separation is between tyre surface and soil surface.

The shear stress displacement curves for the soil-soil and rubber-soil modes are shown in Figs. 7 and 8 respectively. In both figures it can be seen that the shear stress values increase with increasing displacement up to a certain displacement value, after which the shear stresses remain nearly constant. It may also be noted that both the steepness of the stress-displacement curves and the maximum val-

ues of shear stresses increase with increasing normal stress for both soil-soil and rubber-soil model.

Prediction

With the soil tests and tyre-soil interface test results, the tyre property test results can now be introduced to complete implementation of the prediction model. The results of the compression tests on a Goodyear 7.00-16LT (treaded tyre), with 34.5, 103.4 and 310.4 kPa inflation pressures on a rigid surface is shown in Fig. 9. The comparison between the experimental results of tow bin test and the proposed model is shown in Fig. 10 for 34.5 and 310.4 kPa inflation pressure and 1.7 kN axial wheel load. The torque versus slip is presented in Fig. 10a, while the drawbar pull versus slip is presented in Fig. 10b. It can be seen that there is a good agreement between the predicted and the experimental results. With higher inflation pressure both torque and drawbar pull decreased as a function of slip.

A parametric study has been carried out to investigate the effect of different axial wheel loads and inflation pressure on the performance of wheeled vehicles. Torque variation with slip for various inflation pressure and axial wheel load is presented in
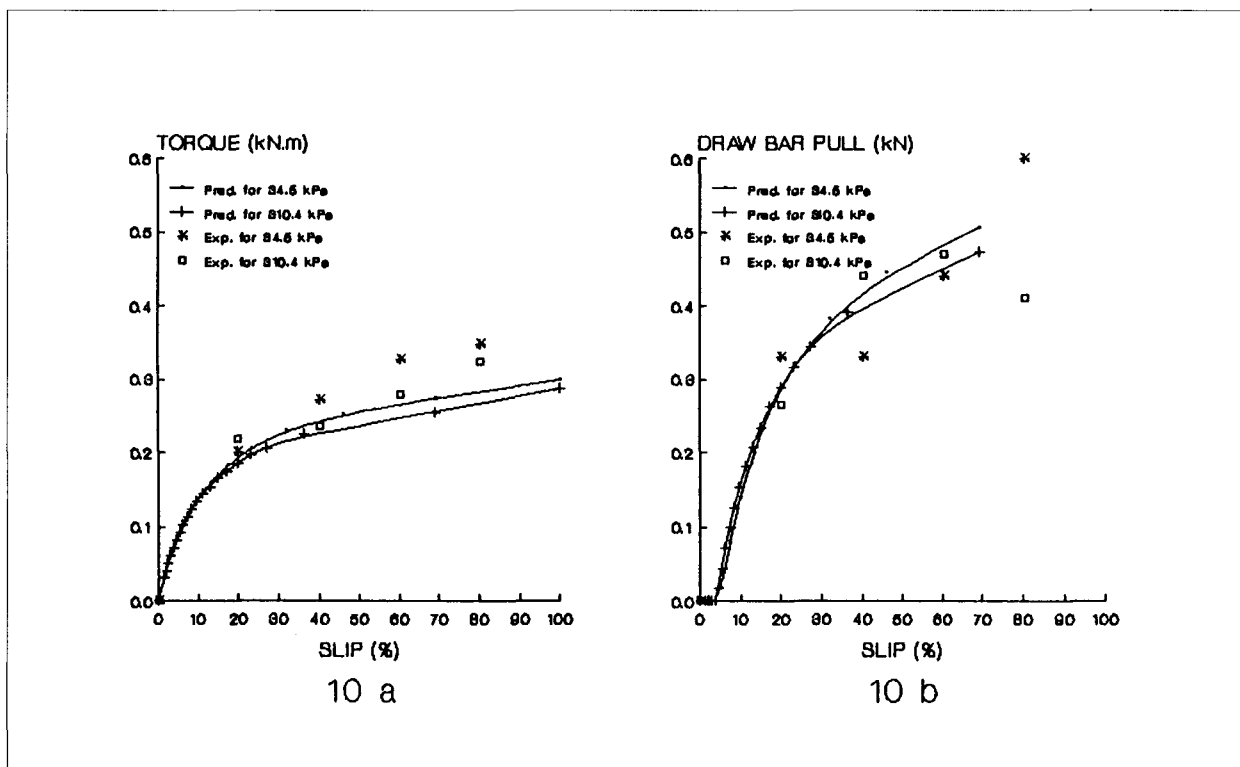
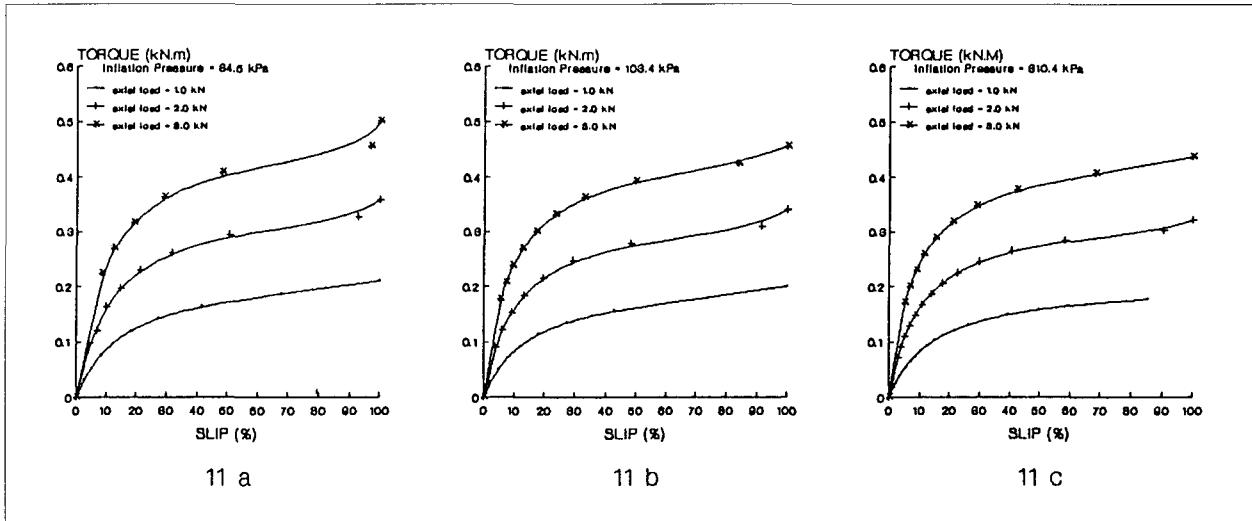**Figure 10.** Comparison between Predicted and Experimental Results for Axial Wheel Load = 1.7 kN.

Figure 11. Variation of Torque with Slip for Various Inflation Pressures and Axial Wheel Loads.

Fig. 11. It can be seen that for the same slip, torque increases with the increase in axial wheel load, which can be attributed to the increase in contact length and sinkage, while, with the increase in inflation pressure, the torque decreases for the same axial wheel load and slip, which is attributed to the decrease in contact length and sinkage with an increase in inflation pressure.

For various inflation pressures and axial wheel loads, the drawbar pull-slip relationships are shown in Fig. 12. For the same axial wheel load, the drawbar pull increases with the increase in slip, while, with the increase in axial wheel load, the drawbar pull does not appear to increase or decrease accordingly.

This can be explained by the fact that the drawbar pull is calculated by subtracting the motion resistance from the tractive force; therefore the drawbar pull will be the resultant effect of both parameters. It can be seen that the motion resistance as well as the tractive force increases with the increase in axial wheel load due to the increase in both contact length and sinkage. However, the proportional increase in motion resistance as well as tractive force with the increase in axial wheel load is not the same, hence resulting in the undefined pattern of the drawbar pull increase with slip.

Furthermore, for the same axial wheel load the drawbar pull decreases with the increase in inflation
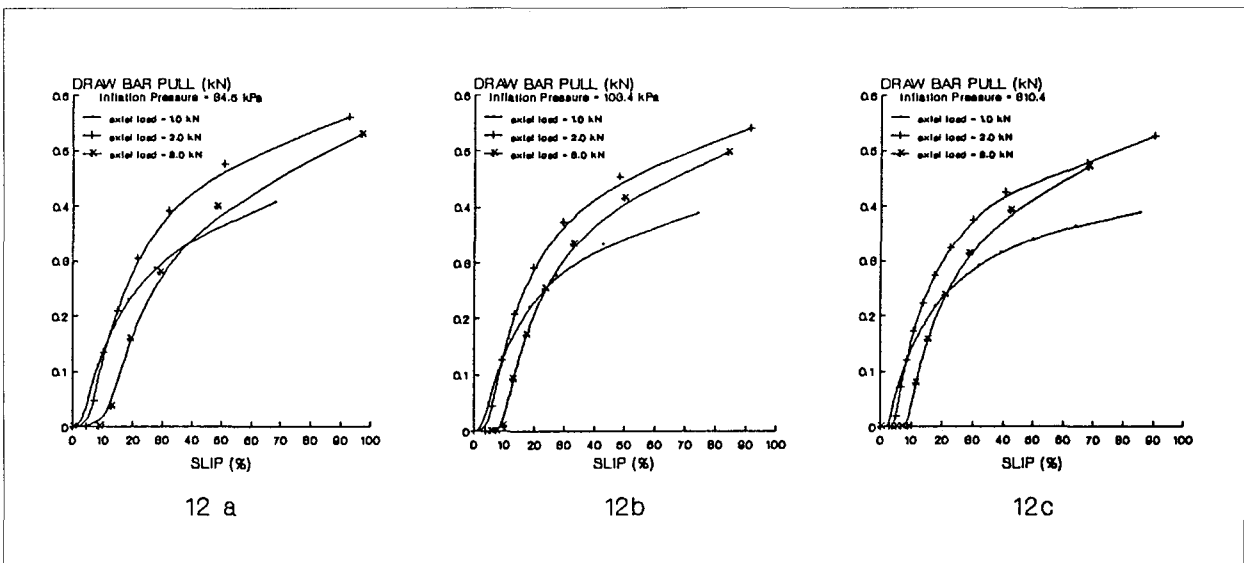

Figure 12. Variation of Drawbar Pull with Slip for Various Inflation Pressures and Axial Wheel Loads.

pressure due to the increase in motion resistance.

Additionally, for the various inflation pressures, the tractive efficiency-slip relationships are presented in Fig. 13. For the same inflation pressure, the tractive efficiency decreases with the increase in axial wheel load due to the increase in motion resistance. It can be seen also that the tractive efficiency increases with slip up to a certain limit, after which the tractive efficiency decreases sharply. Furthermore, results from Fig. 13 indicate that, for this type of soil, the vehicle can perform very well within a 10 to 20 percent slip range.

The parametric study has demonstrated the effect of axial wheel load and inflation pressure on the performance of a wheeled vehicle on soft soil. For this specific type of soil, the highest tractive efficiency can be achieved by having lower axial wheel

salient features are evident from the numerical calculation:

(1) contact length is affected by the vertical load, soil stiffness and inflation pressure;

(2) there is a threshold torque below which the vehicle cannot move because the input energy is less than internal energy of the system;

(3) wide and soft tyres (low inflation pressure) help the vehicle to move with less slip due to reduction in induced shear stresses, and

(4) prudent selection of inflation pressures according to soil type is a very promising way to guarantee good vehicle motion.

REFERENCES

[1] Boyd, C.W. and Windisch, S.J. (1966) "A Technique for Measuring Deformations within a Sand under Controlled Wheels Loads" Proc. 2nd Int.
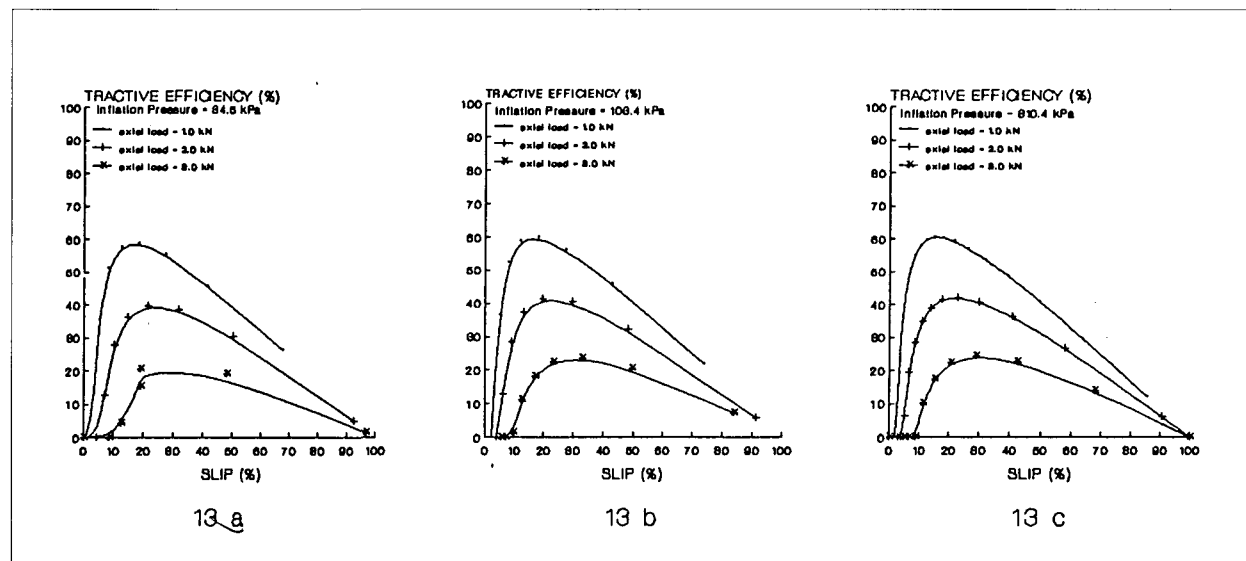

Figure 13. Variation of Tractive Efficiency with Slip for Various Inflation Pressures.

load and lower inflation pressure.

CONCLUSION

Based on energy principles as well as a quasi-static moving boundary displacement method, a model for prediction of vehicle performance has been derived. For a given condition of both tyre and terrain characteristics, the contact length, the slip rate, the tractive efficiency and the drawbar pull can be calculated. The effect of tread configuration is also included in the slip rate calculation. The following

Conf. ISTVS, Quebec, pp. 193-197.

[2] Karafiath, L.L. and Nowatzki, E.A. (1978) "Soil mechanics for Off-Road Vehicle Engineering" Trans-Tech. Publ., Germany, 515 p.

[3] Kondner, R.L. (1963) "Hyperbolic Stress-Strain Response: Cohesive Soils" ASCE, J. of SM&FE, Vol. 89, No. 2M1, p. 115.

[4] Xu, D.M., Yong, R.N., Mohamed, A.M.O., and

Irwin, G.J. (1990) "Tyre Performance Prediction Using a Quasi-Static Moving Boundary Displacement Method" Proceedings of the IASTED International Symposium Modelling, Simulation and Optimization, Montreal, Canada, May 22-24, ed. Jacyno, 2, pp. 107-110.

[5] Yong, R.N., and Webb, G.L. (1969) "Energy Dissipation and Drawbar Pull Prediction in Soil-Wheel Interaction" Proc. 3rd Int. Conf. ISTVS, Essen, Vol. 1, pp. 93-142.

[6] Yong, R.N., and Fattah, E.A. (1976) "Prediction of Wheel-Soil Interaction and Performance Using the Finite Element Method" J. Terramechanics, Vol. 13, No. 4, pp. 227-240.

[7] Yong, R.N., Fattah, E.A., and Boonsinsuk, P. (1978) "Analysis and Prediction of Tyre-Soil Interaction and Performance Using Finite Elements" J. Terramechanics, Vol. 15, No. 1, pp. 43-63.

[8] Yong, R.N., Boonsinsuk, P., and Fattah, E.A. (1980) "Tyre Load Capacity and Energy Loss with Respect to Varying Soil Support Stiffness" J. Terramechanics, Vol. 17, No. 2, pp. 131-147.

[9] Yong, R.N., Fattah, E.A., and Skiadas, N. (1984) "Vehicle Traction Mechanics" Elsevier Science Publishers, Netherlands, 306 p.

ACKNOWLEDGEMENTS